Preprints.org

Article

Analysis of FOXP3 Gene Expression in OVCAR3 Cell Line After Rosmarinic Acid and Doxorubicin Treatment

Veysel Toprak , İlhan Özdemir , Şamil Öztürk , Orhan Yanar , Yusuf Ziya Kızıldemir , Mehmet Cudi Tuncer *

Article

Analysis of FOXP3 Gene Expression in OVCAR3 Cell Line After Rosmarinic Acid and Doxorubicin Treatment

Veysel Toprak [1], İlhan Özdemir [2], Şamil Öztürk [3], Orhan Yanar [4], Yusuf Ziya Kizildemir [5] and Mehmet Cudi Tuncer [6,*]

[1] Private Metrolife Hospital, Şanlıurfa, Turkey
[2] Department of Gynecology and Obstetrics, Faculty of Medicine, Atatürk University, Erzurum, Turkey
[3] Vocational School of Health Services, Çanakkale Onsekiz Mart University, Çanakkale, Turkey
[4] Private Nev Hospital, Şanlıurfa, Turkey
[5] Şanlıurfa Training and Research Hospital, Şanlıurfa, Turkey
[6] Dicle University, Faculty of Medicine, Department of Anatomy, Diyarbakir, Turkey
[*] Correspondence: drcudi@hotmail.com; Tel.: +90-412-2488001 (Ext. 4539) or +90-532-2744926; Fax: +90-412-2488440

Abstract: Aim: Ovarian cancer is the leading cause of gynecological cancer deaths worldwide. Treatment methods are listed as surgery, chemotherapy and radiotherapy depending on the stage of the cancer, but developing resistance to chemotherapy increases the need for alternative agents that act on the same pathways. In this study, the effects of rosmarinic acid (RA) and doxorubicin (DX) on the activation of FOXP3, an important tumor suppressor gene, in OVCAR3 cells were examined. **Materials and Methods:** In the study, human ovarian adenocarcinoma cell line was used. MTT test was applied to determine the effect of rosmarinic acid and doxorubicin on the proliferation of OVCAR3 cells. Expression levels of FOXP3 for cell proliferation and Capase-3 for Apoptosis were determined by qRT-PCR and Western blot analysis. Wound healing model was applied to determine metastasis. The results were evaluated with one-way ANOVA in SPSS 20.0 program as $p \leq 0.05$. **Results:** It was determined that rosmarinic acid alone and in combination with doxorubicin inhibited the proliferation of OVCAR3 cells in a time- and dose-dependent manner for 24, 48 and 72 hours, and caused the cells to die by causing them to undergo apoptosis. It was observed that Caspase-3 expression increased approximately tenfold in OVCAR3 cells, while FOXP3 expression increased only in RA treatment and was downregulated in DX and RA+DX treatments. **Conclusions:** According to the results of our study, it was observed that many steps of the signaling pathways related to proliferation, migration and apoptosis were affected by the combination of RA and DX in OVCAR3 cells. This shows that RA will gain an important place in cancer treatment with more comprehensive studies.

Keywords: Ovarian cancer; FOXP3; apoptosis; rosmarinic acid; tumor supressor

1. Introduction

Ovarian cancer is the third most common gynecological malignancy affecting women in the world. However, it ranks first among cancers in terms of mortality rate. Moreover, its non-symptomatic course, late diagnosis, and frequent recurrence are other disadvantages [1–3]. When diagnosed, peritoneal involvement and intraperitoneal metastasis usually occur together [2,4]. Ovarian cancer cells can easily develop resistance to traditional chemotherapeutics, and this contributes to an increase in relapses [5]. Although the characteristic etiology for ovarian cancer is a question mark, since these cancers occur in advanced stages, the molecular mechanisms underlying the development are unknown.

Today, medicinal plants have become important not only as food supplements but also for pharmacological and drug development. Rosmarinic acid is widely found in many plants and is a powerful polyphenol. It is found in high concentrations especially in plants such as rosemary and sage. It is one of the components that give these plants their aromatic properties [6]. RA exhibits very strong antioxidant properties, and this feature is stronger than that of vitamin E. While RA reduces the risk of chronic diseases such as cancer, it prevents cellular damage caused by free radicals [7]. In an in vivo study conducted with various different doses of RA, they investigated its mutagenicity against the antitumoral agent doxorubicin using the micronucleus method in the blood cells of Swiss mice. Mice treated with three different doses of RA showed antioxidant capacity with results close to the control group. A significant increase in micronucleus frequency was detected in subjects given DX in combination with RA. Although the mechanism explaining the protective effect is not fully known, it has been reported that RA exhibits strong antioxidant activity in DX toxicity [8].

The master transcription factor forkhead box protein P3 (FOXP3) characterizes nTregs produced after activation of naive T cells in the presence of TGFβ [9]. The transcription factor FOXP3 belongs to the family of forkhead-winged helix transcription factors. As a broad regulator of gene expression, it plays a central role for the identity and function of the most widely recognized and well-studied subset of immunoregulatory T cells [10]. Tregs work to suppress an autoimmune response in the body and play an important role in carcinogenesis, and in cancer this action allows cancerous cells to escape the anti-tumor response and can suppress anti-tumor immunity [11].

In this study, a cell line (OVCAR3) belonging to the epithelial subtype, one of the most common types of ovarian cancer, was used. The anti-cancer effects of single and combination application of Doxorubicin agent and Rosmarinic acid compound were evaluated. Decreasing long-term survival rate and recurrence have increased the interest in alternative drugs that are less toxic and more anticancer effective for ovarian cancer. Moreover, it is important to investigate new drugs such as DX, which work in a similar way to chemotherapy drugs and offer additional treatment options for ovarian cancer. In this study, the anticancer properties of Rosmarinic acid, a natural antioxidant, were investigated.

2. Materials and Methods

2.1. Cell culture

This study was performed using the human ovarian carcinoma cell line NIH:OVCAR-3 (HTB-161™). OVCAR-3 cells were cultured using RPMI 1640 containing 10% FBS for the medium, and the cells were grown in a sterile incubator at 37°C and 5% CO_2. In all steps of the studies, cells were used starting from the 5th passage and the study was completed at most at the 20th passage.

2.2. Cell viability

To determine the IC50 doses of Rosmarinic acid and Doxorubicin, OVCAR-3 cells were seeded in 96-well culture dishes. At the end of one night, 9 different concentrations of Doxorubicin in the dose range of 0.5-50 μM and Rosmarinic acid in the dose range of 10-1000 μM, obtained as a result of serial dilution, were applied. In MTT cell viability analysis after 24, 48 and 72 hours, anticancer agents and vehicle control group were seeded in 6 wells. After incubation, cell survival analysis was performed by MTT test. In the first step, 5 mg/ml "Yellow tetrazolium MTT (3-(4, 5-dimethylthiazolyl-2)-2,5-diphenyltetrazolium bromide)" test solution was added to each well as 20 μl. In the second step, the cells in solution were incubated for 4 hours, and the cell medium was completely removed after the incubation. In the third step, ultrapure DMSO (Merk, USA) was added at 200μl/well and kept in the incubator in a dark environment for 4 hours. At the end of the period, the plates were read spectrophotometrically in a Multiskan GO microplate reader (Thermo Scientific, USA) at wavelengths of 492, 570 and 650 nm. The group treated with vehicle was taken as control and the obtained value was taken as 100% viability. IC50 values for each cancer cell line and anticancer agents in the control and treatment groups were calculated using the SPSS 20 statistical package program.

2.3. Metastasis analysis

For the wound healing model, OVCAR-3 cells were seeded in 6-well cell plates with approximately 200.000 cells per well. When the cells in the wells were 90% confluent, a wound was made on the cells with a sterile micropipette tip of 200 μl volume. After wound opening, shielded cells were removed by washing with PBS (Gibco, USA). Then, serum-free medium containing vehicle, 72-hour IC_{50} value of DX, IC_{50} RA and IC50 DX+RA agents was added to each well. Cells were imaged using the Thermo EVOS® FL Imaging System at hour 0, and the wound model was checked until the wound in the control group was completely closed. The study was terminated at the 36th hour when the wound in the control group was 90-100% closed, and the wound healing rates of the groups were photographed. In cell migration analysis, wound opening was measured using Image J software. In a total of 3 wells, 4 measurements were made in the widest and narrowest areas of each well, and a total of 12 data were used for each group. The value obtained from the control group was taken as 100% cell migration and comparative rates were determined.

2.4. Apoptotic staining

In OVCAR-3 cells, nuclear morphologies and apoptotic cells after apoptosis caused by DX and RA agents were detected with NucBlue® Live ReadyProbes® Reagent (Thermo Scientific, USA) specific dye. In this context, OVCAR-3 cells were planted in 24-well plates with 50,000 cells in each well and incubated. The next day, vehicle material, 72-hour IC50 RA, IC50 DX, IC50 DX+RA agents were applied to the wells to form groups. Staining was then performed directly on live cells according to the kit protocol, and the cells were incubated at 37°C for 30 minutes. At the end of this period, the plates were photographed using the Thermo EVOS® FL Imaging System using bright field and fluorescence mode with a 20x objective and a DAPI filter.

2.5. Gene expression analysis

Total RNA isolation was performed using the Purelink RNA mini kit (Thermo, USA). Total RNA concentration and purity in the samples were determined using the Optizen NanoQ microvolume spectrophotometer (Mecasys, South Korea). cDNA synthesis was performed with the High-Capacity cDNA Reverse Transcription Kit (Life Technologies, USA) using 100 ng total RNA. Gene expression levels in cDNA samples were measured with a real time PCR system (PikoReal™ Real-Time PCR System, Thermo Scientific) using the SYBR Green/ROX qPCR Master Mix (2X) (Thermo Scientific) kit. Using the threshold cycle (CT) values measured with the device, the relative gene expression levels of the genes belonging to FOXP3 and CASP3 were calculated as fold change according to the 2-ΔΔCT method. According to this method, the following formulations were used; ΔCT = CT (target gene)-CT (β-actin) Δ(ΔCT) = ΔCT (control group)-ΔCT (treatment group). Fold change = 2-ΔΔCT Primer sequences used in the study are given below. The specificity of the primers to the target gene was confirmed using the NCBI Primer-BLAST program.

FOXP3: F: GTGGCCCGGATGTGAGAAG, R: GGAGCCCTTGTCGGATGATG
CASP3: F: GGTATTGAGACAGACAGTGG, R: CATGGGATCTGTTTCTTTGC
β-Actin: F: CCTCTGAACCCTAAGGCCAAC, R: TGCCACAGGATTCCATACCC
GAPDH; F: CGGAGTCAACGGATTTGGTCGTAT, R: GCCTTCTCCATGGTGGTGAAGAC

2.6. Western blot

For protein analysis, OVCAR-3 cells were seeded in 75 cm2 culture flasks and incubated until the logarithmic phase was reached. When it came to the logarithmic phase, control, IC50 DX, IC50 RA were applied individually and in combination. Protein isolation was performed after 72 hours. After removing the medium from the flasks, the cells were homogenized in 500 μl of RIPA lysis buffer (RIPA Lysis Buffer System, sc-24948, Santa Cruz, USA) under cold conditions with a Daihan 15D tissue homogenizer (27,000 rpm). The homogenate was centrifuged at 14000 g for 20 min. Protein amounts (approximately 1.2-1.6 mg/ml) were determined using nano spectrophotometer Optizen Nano Q, Mecasys, Korea. 6.5 μl of equal proteins were added to strips kept in cold conditions. Then,

2.5 µl LDS Sample Buffer (4X) BoltTM and 1 µl Sample Reducing Agent (10X) BoltTM were added. The ready samples were denatured in the PCR device at 80ºC for 12 minutes. After denaturation, the samples were kept on ice for a while. Next, proteins were loaded onto NuPAGE® Bis-Tris polyacrylamide gel (10%) and electrophoresis was performed. Using Western Breze brand ready-made kits, blotting and membrane transfer were performed with the iBlot 2 (Life Technologies) system. After blotting, the proteins were treated with specific primary antibodies of FOXP3 Antibody [C3], Cterm (GeneTex, CAT no: GTX107737), Beta actin Antibody (Invitrogen, CAT no: MA1-140) and the antibodies were labeled with appropriate secondary antibodies and Micro ChemiDoc (DNR Bio-Imaging Systems Ltd, USA) gel imaging system and band intensities were calculated using GelQuant software.

2.7. Protein-Protein interaction (PPI) analysis

PPI data were retrieved from the STRING database. The STRING database provides descriptions of protein-protein interactions (PPIs) as well as confidence intervals for data scores. A confidence score greater than or equal to 0.4 was chosen to construct the interaction network of proteins with target genes.

2.8. Enrichment analysis

Data on the functional annotation of genes and the canonical pathways associated with the strong connections established with these proteins were obtained using the ShinyGO 0.80 program.

2.9. GO functional enrichment analysis

Three types of Gene Ontologies (GO) were performed on possible target genes: cellular component (CC), biological process (BP) and molecular function (MF). The SRplot bioinformatics program was used to evaluate these data.
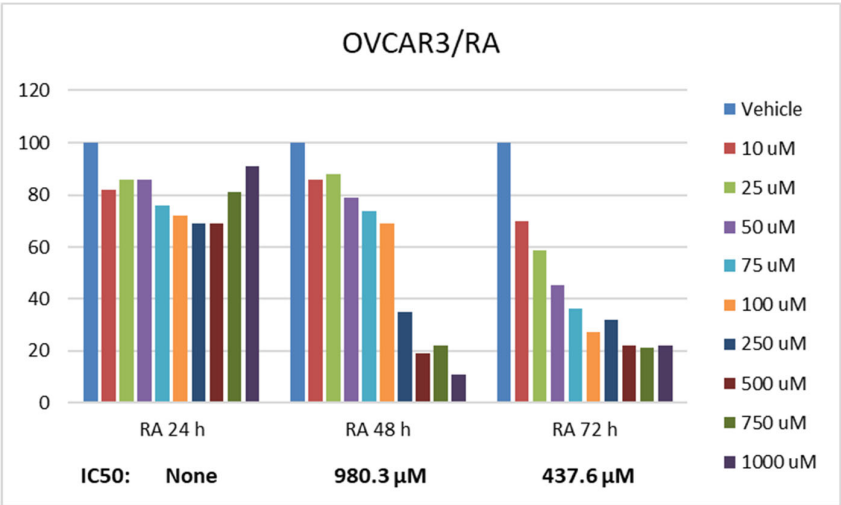
2.10. Statistical analysis

The difference between the averages of cell viabilities determined by the MTT test and expression values obtained from qRT-PCR studies was determined by one-way ANOVA. The groups within which the averages fell were determined using the Tukey HSD test. Comparisons between two groups were determined by the independent sample t test or Mann Whitney U test, depending on the homogeneity of the data. Analyzes were performed with SPSS 20 (IBM, USA) program and $p \leq 0.05$ was used.

3. Results

### 3.1. Cell viability and inhibitory concentration

Statistically significant differences were determined when the basal proliferation rate of OVCAR3 cells was compared between RA and DX treatments. The inhibitory effect of RA and DX on the proliferation of OVCAR3 cells increased depending on time and concentration (Figures 1 and 2). The IC50 of RA was measured as none at the 24th hour, 980.3 µM at the 48th hour, and 437.6 µM at the 72nd hour, respectively (Figure 1). The IC_{50} value of DX could not be measured at the 24th hour, but was measured as 5.32 µM and 1.23 µM at the 48th and 72nd hours, respectively (Figure 2).

Figure 1. Effect of 24, 48 and 72 hour treatment of RA in the concentration range of 10-1000 μM. Inhibition concentration (IC50) was calculated by Probit analysis. * data are statistically significant compared to means, one-way ANOVA, Tukey HSD test, $p \leq 0.05$.

The therapeutic potential of RA has been demonstrated in many cancers, but its anti-cancer effect in OCVAR3 cells remains to be determined. Cell viability rate was determined by 24, 48 and 72 hours of RA and DX treatment of human ovarian adenocarcinoma cells. When we look at the results; It was observed that the increase in cell proliferation was very limited at the 24th hour of DX application, but showed a concentration- and time-dependent decrease at the 48th and 72nd hours (Figure 1). OVCAR3 cells decreased in the RA-treated group depending on the RA concentration of the cells. It was determined that the cells that initially increased in the 24th hour of RA treatment rapidly lost their viability depending on concentration and time. Regardless of the treatment duration, it was observed that cell activity decreased below 60% when the RA concentration reached 1000 μM/L. At the 72nd hour, cell activity decreased significantly for both RA and DX treatments, regardless of concentration. Therefore, gene and protein analyzes in the study were performed according to IC_{50} RA and IC_{50} DX incubation (Figure 2).
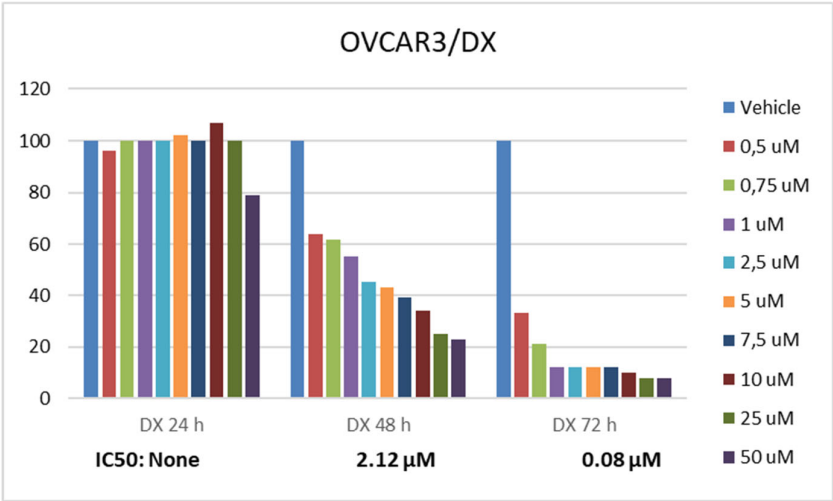

Figure 2. Effect of 24, 48 and 72 hour treatment of DX in the concentration range of 0.5-50 μM. Inhibition concentration (IC50) was calculated by Probit analysis. *data are statistically significant compared to means, one-way ANOVA, Tukey HSD test, $p \leq 0.05$.

3.2. Metastasis findings

Metastasis rate was determined by wound healing test in OVCAR-3 cells. The time when the wound was created was taken as 0, and the time when the control group cells completely closed the area was considered the closing time. Control group cells completely covered the area after 36 hours. At the same time, treatment groups were terminated and the area covered by the cells was photographed. Recovery in OVCAR-3 cells was evaluated as % wound size and cell migration compared to the control group $t = 0$. According to the data obtained, the wound area closed with nearly 100% cell migration after 36 hours in the control group. In the DX treatment group, it was observed that the wound area, which had no cells at hour 0, closed by 46% after 36 hours (Figure 4). In the RA treatment group, it was observed that the wound area, which was completely open at hour 0, was closed by 36% cell migration after 36 hours. In the DX+RA treatment group, cell migration was found to be 22% at the end of 36 hours. Consistent with these results, it was determined that the combination of DX+RA provided higher migration in OVCAR-3 cells than the application of DX and RA alone (Figure 3).
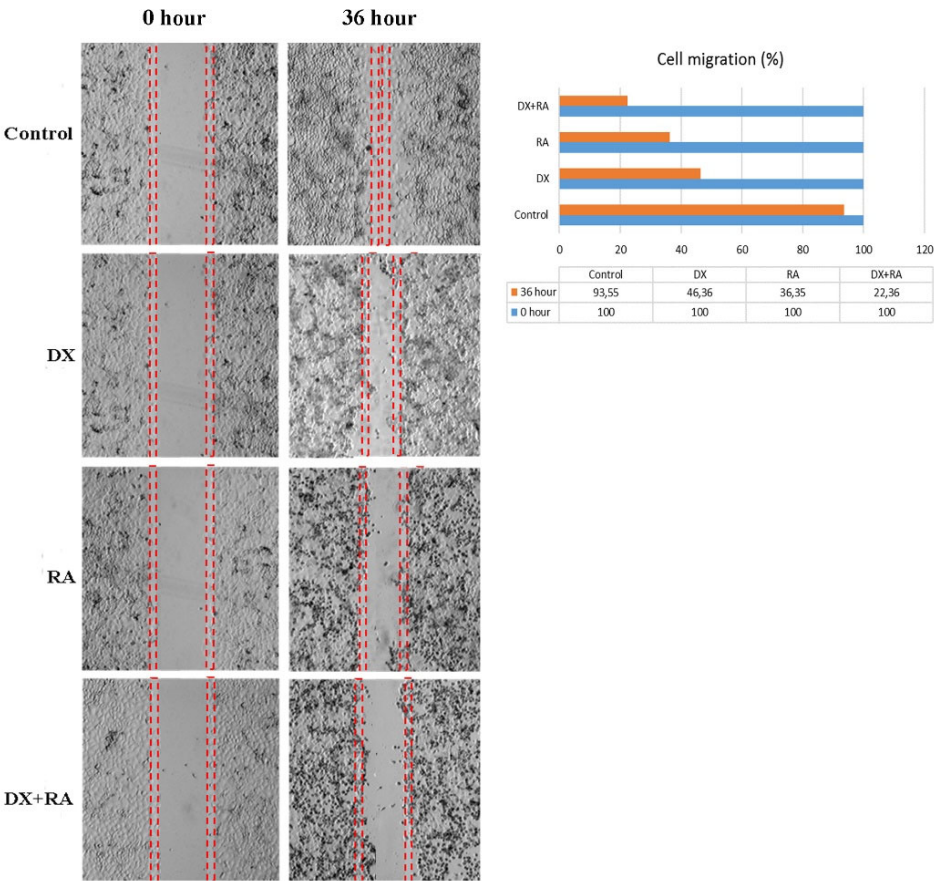
Figure 3. Cell migration rate and % wound closure determined by wound healing assay (for 36 hours) in OVCAR-3 ovarian carcinoma cell populations treated with vehicle control, DX, RA, DX+RA IC$_{50}$.
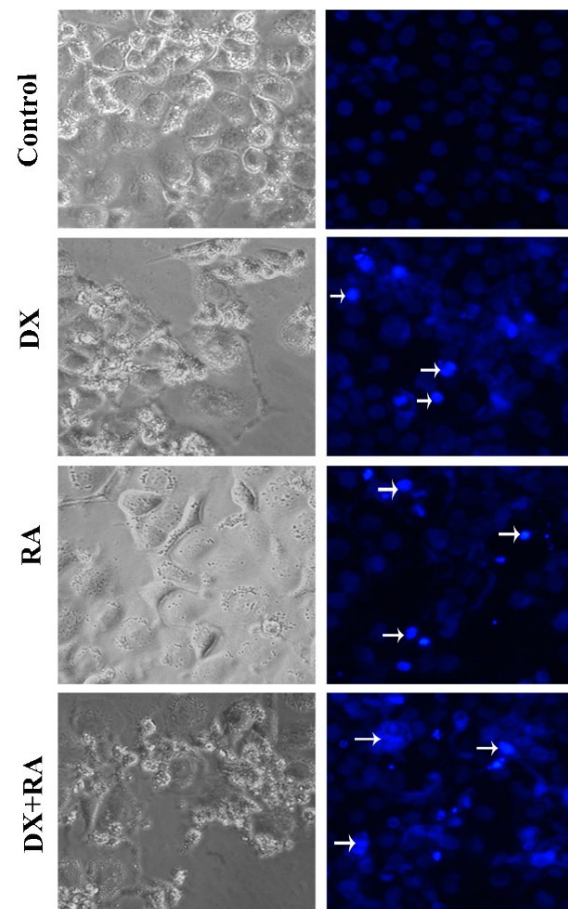
Figure 4. Apoptotic body formation (arrow: apoptotic cell, magnification: X20).

3.3. Apoptotic findings

Apoptotic Nucblue staining was performed to determine apoptosis and reveal the apoptotic role of DX and RA. While the morphology and nuclear structure of the cells in the control group appeared normal, it was determined that the cells in the RA and DX treatment groups gained a bright appearance due to the deterioration of the nuclear structure. In this staining, it was seen that the highest apoptotic cell death occurred only in the DX and DX+RA treatment groups (Figure 4).

3.4. qRT-PCR (FOXP3, CASP3) findings

According to the expression results of genes that play an important role in suppressing the proliferation of cancer cells and driving them to apoptosis, statistically significant differences were detected in FOXP3 and CASP3 gene expressions. A significant difference was detected in FOXP3 gene expression between the control and all treatment groups with $p \leq 0.05$. It was observed that gene expression decreased in the control group and in the DX and DX+RA groups and the significance was $p \leq 0.0001$, and FOXP3 expression increased in the RA treatment group, creating a significant difference between the control group and the control group. Additionally, no significant difference was observed between the DX treatment group and the DX+RA treatment group (Figure 5). Again, when the expressions of genes regulating apoptosis were evaluated, CASP3 showed a significant increase in all groups compared to the control, while the highest increase was seen only in RA and DX+RA treatments. Compared to the control group, no statistically significant difference was detected between the DX and RA treatment groups alone (Figure 5).
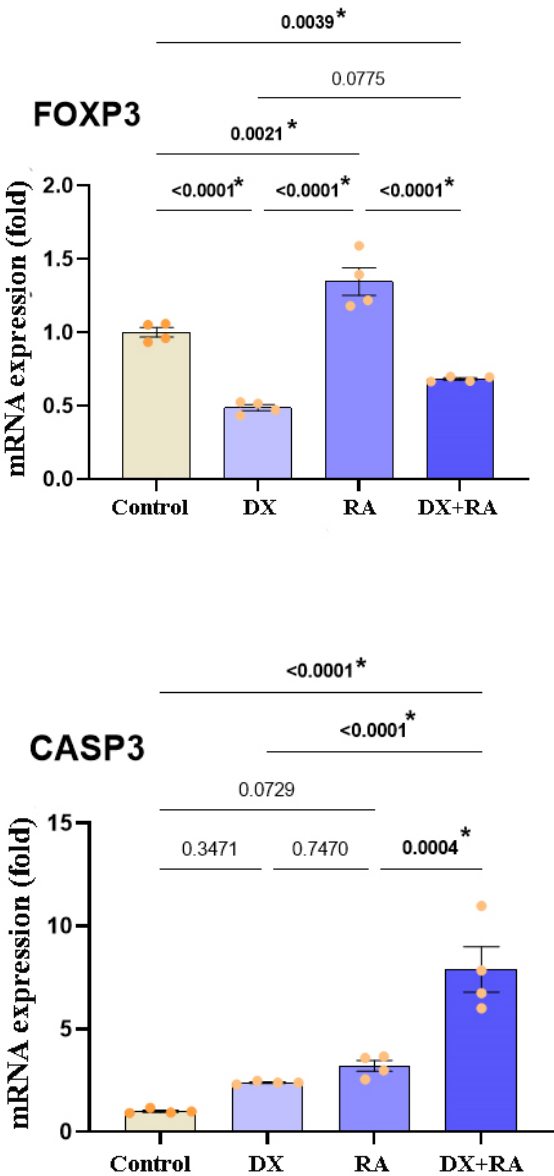
Figure 5. Relative fold values of FOXP3 and CASP3 gene expressions in OVCAR-3 cell lines (data in multiple control with β-actin and GAPDH mRNA level). method, n=4 data mean±SH), * means are statistically different, one-way ANOVA, Tukey HSD test, p values are given in the graph.

3.5. Western blot findings

FOXP3 and CASP3 protein levels were determined by western blot technique. Results parallel to qRT-PCR findings were obtained. While FOXP3 was highest in the RA treatment group, CASP3 protein amount showed the highest increase in the DX+RA group. While FOXP3 was inhibited except in the RA group, CASP3 was increased in the treatment groups (Figure 6).
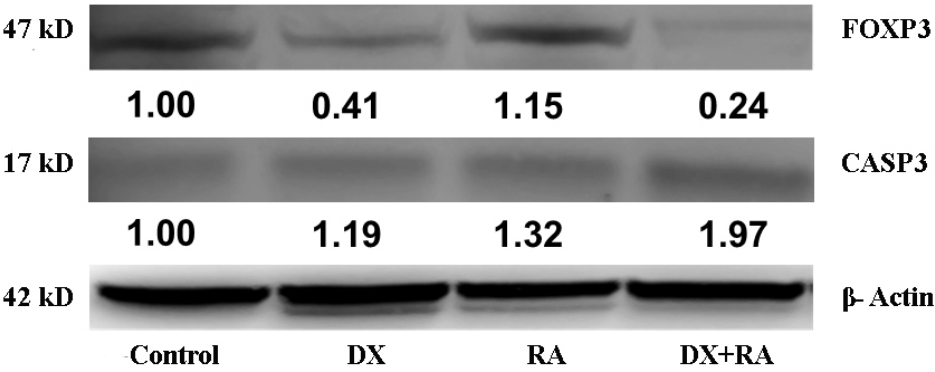
Figure 6. Western blot analysis of FOXP3 and CASP3 expression in OVCAR3 cell line.

3.6. PPI analysis findings

Predictions from STRING analysis were used to depict protein interactions. The visualization showed 11 nodes and 46 edges (Figure 7). Based on nodal degree, the following genes were identified as the top 10 central genes: STAT3, IFNG, NFATC2, RUNX1, IL2, RORC4, CTLA4, HIF1A, CD4, KAT5. These targets are hypothesized to be the primary targets in ovarian cancer of RA.
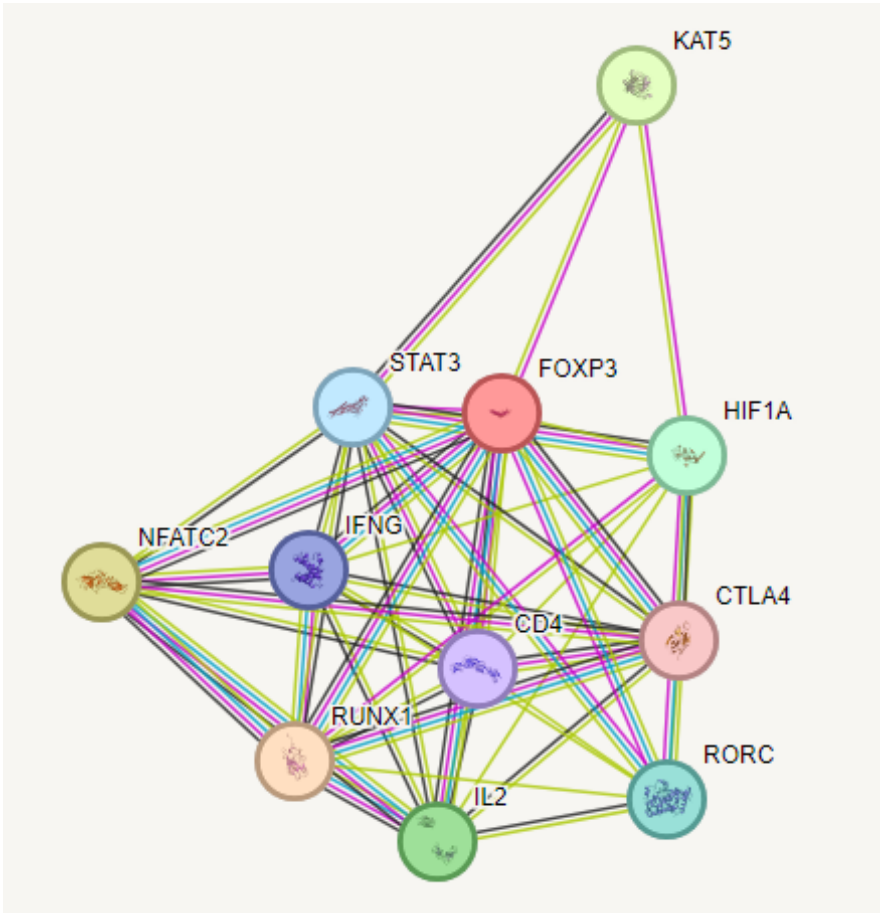
Figure 7. PPI and interaction between various genes of ovarian cancer.

3.7. KEGG pathway enrichment analysis

KEGG pathway enrichment analysis of target genes was performed with Shiny 0.80 program. The findings showed that 90 genes were involved in the enrichment process and 50 pathways were cancer-related, exhibiting a significant correlation with target genes ($P < 0.05$). Basically Th17 cell differentiation, Th1 and Th2 cell differentiation, Inflammatory bowel disease, PD-L1 expression and PD-1 checkpoint pathway in cancer, T cell receptor signaling pathway, Chagas disease, C-type lectin receptor signaling pathway, Osteoclast differentiation, IL -17 signaling pathway, AGE-RAGE signaling pathway, the top 10 pathways that occur in diabetic complications are shown (Figure 8).
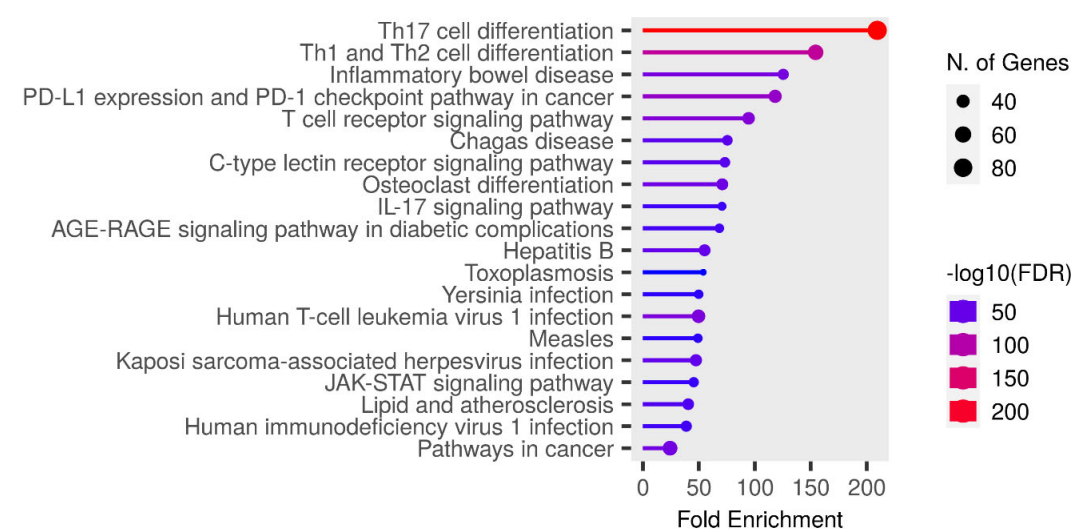

Figure 8. Enrichment analysis for the 90 common compound targets.

3.8. GO functional enrichment analysis findings

Analysis findings show only important functions (Figure 9). Target genes were found to be involved in various cellular components in the BP category, such as helper T cell differentiation, regulation (Figure 9). In terms of cellular components, target genes have been implicated in the regulation of transcription from the RNA polymerase II promoter, signal transduction, and as a complex regulator of chromatin and transcription. It was found that the MF category exhibited roles such as DNA transcription binding and binding of RNA polymerase to DNA (Figure 9).
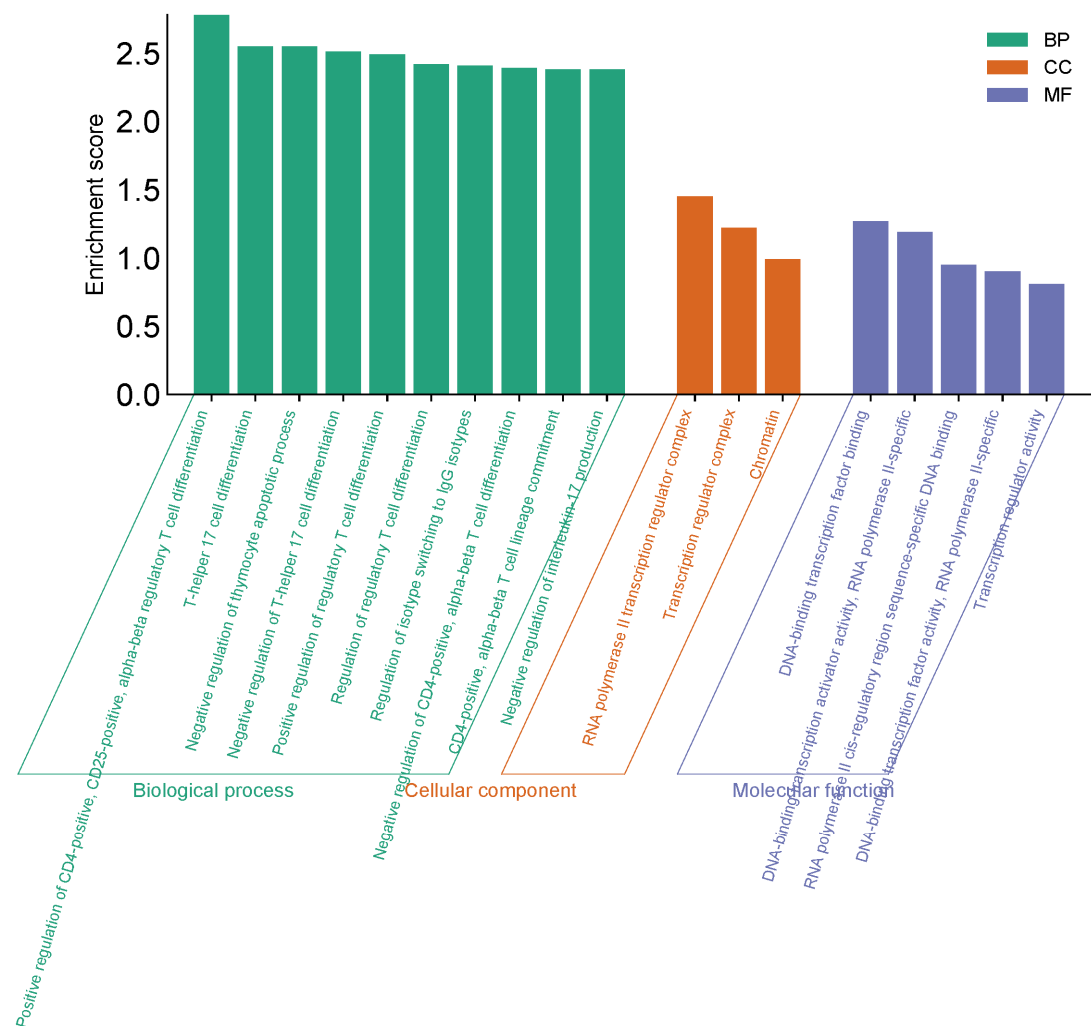
Figure 9. GO (Biological process, molecular function, and cellular component) analysis.

4. Discussion

In this study, the effect and potential mechanisms of RA on OVCAR3 cells were investigated. It was revealed that RA could inhibit cellular proliferation and migration on OVCAR3 cells, a human ovarian carcinoma cell line, and increase apoptosis and DX sensitivity in OVCAR3 cells. RA also downregulated FOXP3 and upregulated CASP3 expression level in OVCAR3 cells, suggesting that it has anticancer potential in ovarian carcinoma and that FOXP3 activation may be important in tumor inhibition.

Ovarian cancer is the leading cause of gynecological cancer deaths in developed countries and is often diagnosed at an advanced stage [13]. Current treatment for advanced ovarian cancer is cytoreductive surgery and chemotherapy [13–15]. It has a high response rate to treatment, but it is a difficult disease to combat because most of them relapse and resistance to chemotherapy develops [14]. Therefore, alternative approaches are needed for early diagnosis and effective treatment of ovarian cancer. Over the last three decades, numerous preclinical and clinical studies have been conducted to identify and develop potential drug candidates [16].

Plant-derived compounds have recently gained importance as alternatives to chemotherapy due to their strong activities against carcinogenic cells. Promising drugs have begun to be produced for many types of cancer, especially from natural compounds such as rosmarinic acid, alpha lipoic acid, ascorbic acid and curcumin [17–19]. The main goal is to get rid of the side effects of current

chemotherapy. Antioxidants have an important place at this point. Exogenous antioxidants show varying effectiveness in eliminating oxidative stress in vivo. Its effects vary depending on the type of antioxidant, its biopharmaceutical properties, its absorption at the site of action, and its suitability for oxidative stress nature [19]. Plant species where RA is found; Rosmarinus officinalis, Perilla frutescens L. and Salvia officinalis L. It appears as a derivative of caffeic acid and 3,4-dihydroxyphenyllactic acid found in these plants [20]. There are many studies on the numerous effects of RA, such as antitumor, anti-inflammatory and antioxidant, and reports on its pharmacological effects [21]. Its inhibitory properties have been described in cancers such as skin, pancreatic and breast cancer [22]. It has also been reported that RA can eliminate multidrug resistance in human gastric cancer cells [23]. Many other studies have also suggested that RA can increase the sensitivity of lung and ovarian cancer cells and exhibit synergistic effects with chemotherapeutics such as cisplatin [24,25]. We confirmed the anticancer effect on human ovarian adenocarcinoma cells, consistent with the results of reports in studies on RA; RA induces apoptosis in OVCAR3 cells and can significantly reduce cell viability. It was also able to block proliferation and metastasis along with DX sensitivity.

Apoptosis is the most common form of self-death of cells, which can occur at different phases in embryonic development, tissue regeneration and regulation, and tumor shrinkage [26]. FOXP3+ regulatory T cells have become therapeutic targets in preventing autoimmune diseases, preventing transplant rejection, and inhibiting the progression of tumors, as they have an active mechanism in immune suppression [27]. While one study reported that FOXP3+ T cells could infiltrate tumors [28], another study failed to support these results [29]. It has also been reported that FOXP3+ T cells are mostly found in the peritumoral region [30]. However, another study observed that these cells were located in different locations [31]. Caspase-3 is a member of a conserved family of proteins that is often involved in sustaining apoptosis in cells that hyperresponsive to specific external or internal stimuli. Furthermore, increasing evidence suggests that caspase-3 plays a key role in the growth and development of both normal and malignant cells in multicellular organisms. This study showed that RA could inhibit the expression of the apoptosis factor CASP3. From here, he showed that RA causes apoptosis through the mechanism of increasing CASP3 gene expression.

When comparing the literature information and our results, it appears that RA plays two opposing roles as a ROS scavenger. It can act as an anti-oxidant or pro-oxidant depending on concentration and redox modulation [30]. While protecting normal cells by eliminating ROS at low doses; At high doses, it induces apoptosis and cytotoxicity in cancer cells (). RA has also been shown to have much stronger anti-cancer effects when combined with chemotherapeutic agents or DOX. In our study, RA also demonstrated its effectiveness on proliferation, migration, and apoptosis through FOXP3 and CASP3 gene expression and protein levels. Additionally, it increased the effectiveness of the RA+DX duo in OVCAR-3 cells, as we expected.

5. Conclusions

The rapid increase in cancer incidence and obstacles to treatment have highlighted the importance of improving the sensitivity of existing chemotherapeutic drugs. Research on more effective and less harmful alternative drug development methods has accelerated. Therefore, RA, an investigated compound, was shown to exhibit anti-tumor activities in FOXP3, a signaling pathway involved in proliferation, migration, and apoptosis. It is thought that future studies will be useful to elucidate this pathway.

References

1. Kuroki L, Guntupalli SR. Treatment of epithelial ovarian cancer. BMJ. 2020;371:m3773.
2. Barani M, Bilal M, Sabir F, Rahdar A, Kyzas GZ. Nanotechnology in ovarian cancer: Diagnosis and treatment. Life Sci. 2021;266:118914.
3. Rojas V, Hirshfield KM, Ganesan S, Rodriguez-Rodriguez L. Molecular Characterization of Epithelial Ovarian Cancer: Implications for Diagnosis and Treatment. Int J Mol Sci. 2016;17(12):2113.
4. Chen SN, Chang R, Lin LT, Chern CU, Tsai HW, Wen ZH, Li YH, Li CJ, Tsui KH. MicroRNA in Ovarian Cancer: Biology, Pathogenesis, and Therapeutic Opportunities. Int J Environ Res Public Health. 2019;16(9):1510.
5. Tarhriz V, Bandehpour M, Dastmalchi S, Ouladsahebmadarek E, Zarredar H, Eyvazi S. Overview of CD24 as a new molecular marker in ovarian cancer. J Cell Physiol. 2019;234(3):2134-2142.
6. Moradi S, Fazlali A, Hamedi H. Microwave-Assisted Hydro-Distillation of Essential Oil from Rosemary: Comparison with Traditional Distillation. Avicenna J Med Biotechnol. 2018 Jan-Mar;10(1):22-28.
7. Hyun Jin C, Yang HS, Choi DS, Byun MW, Kim WG, Jeong Y. Rosmarinic Acid Attenuated SIN-1-induced Cytotoxicity in HepG2 Cells through the HO-1 Induction and Radical Scavenging Activity. Food Science Biotechnology, 2013;22: 549-556.
8. Furtado RA, de Araújo FR, Resende FA, Cunha WR, Tavares DC. Protective effect of rosmarinic acid on V79 cells evaluated by the micronucleus and comet assays. J Appl Toxicol. 2010 Apr;30(3):254-9.
9. Brummelman J, Pilipow K, Lugli E. The Single-Cell Phenotypic Identity of Human CD8+ and CD4+ T Cells. Int Rev Cell Mol Biol. 2018;341:63-124. doi: 10.1016/bs.ircmb.2018.05.007.
10. Lu L, Barbi J, Pan F. The regulation of immune tolerance by FOXP3. Nat Rev Immunol. 2017 Nov;17(11):703-717. doi: 10.1038/nri.2017.75.
11. Plitas G., Rudensky A.Y. Regulatory T Cells in Cancer. Annu. Rev. Cancer Biol. 2020;4:459–477. doi: 10.1146/annurev-cancerbio-030419-033428.
12. Grisham RN, Hyman DM, Iyer G. Targeted therapies for treatment of recurrent ovarian cancer. Clin Adv Hematol Oncol. 2014 Mar;12(3):158-62.
13. Alemzadeh E, Allahqoli L, Mazidimoradi A, Alemzadeh E, Ghasemi F, Salehiniya H, Alkatout I. Deciphering resistance mechanisms and novel strategies to overcome drug resistance in ovarian cancer: a comprehensive review. Oncol Res. 2024 Apr 23;32(5):831-847.
14. Kossaï M, Leary A, Scoazec JY, Genestie C. Ovarian Cancer: A Heterogeneous Disease. Pathobiology. 2018;85(1-2):41-49.
15. Cortez AJ, Tudrej P, Kujawa KA, Lisowska KM. Advances in ovarian cancer therapy. Cancer Chemother Pharmacol. 2018 Jan;81(1):17-38.
16. Ediriweera MK, Tennekoon KH, Samarakoon SR. Role of the PI3K/AKT/mTOR signaling pathway in ovarian cancer: Biological and therapeutic significance. Semin Cancer Biol. 2019;59:147-160. doi: 10.1016/j.semcancer.2019.05.012.
17. Ko YH, Kim SK, Lee SY, et al. Flavonoids as therapeutic candidates for emotional disorders such as anxiety and depression. Arch Pharm Res. 2020;43:1128–1143.
18. Huang L, Chen J, Quan J, Xiang D. Rosmarinic acid inhibits proliferation and migration, promotes apoptosis and enhances cisplatin sensitivity of melanoma cells through inhibiting ADAM17/EGFR/AKT/GSK3β axis, Bioengineered, 2021;12(1):3065-3076.
19. Attia M, Essa EA, Zaki RM, Elkordy AA. An Overview of the Antioxidant Effects of Ascorbic Acid and Alpha Lipoic Acid (in Liposomal Forms) as Adjuvant in Cancer Treatment. Antioxidants (Basel). 2020;9(5):359.
20. Kim GD, Park YS. Jin YH and Park CS: production and applications of rosmarinic acid and structurally related compounds. Appl Microbiol Biotechnol. 2015;99:2083–2092.
21. Swamy MK, Sinniah UR, Ghasemzadeh A. Anticancer potential of rosmarinic acid and its improved production through biotechnological interventions and functional genomics. Appl Microbiol Biotechnol. 2018 Sep;102(18):7775-7793.
22. Messeha SS, Zarmouh NO. Asiri A and Soliman KFA: rosmarinic acid-induced apoptosis and cell cycle arrest in triple-negative breast cancer cells. Eur J Pharmacol. 2020;885:173419.
23. Li F, Fu Y, Jiang D, et al. Reversal effect of rosmarinic acid on multidrug resistance in SGC7901/Adr cell. J Asian Nat Prod Res. 2013;15:276-285.

24. Liao XZ, Gao Y, Sun LL, et al. Rosmarinic acid reverses non-small cell lung cancer cisplatin resistance by activating the MAPK signaling pathway. Phytother Res. 2020;34:1142-1153.

25. Lešnik S, Furlan V, Bren U. Rosemary (Rosmarinus officinalis L.): extraction techniques, analytical methods and health-promoting biological effects. Phytochem Rev. 2021.

26. Wang X, He Z, Liu H et al: Neutrophil necroptosis is triggered by ligation of adhesion molecules following GM-CSF priming. J Immunol, 2016; 197(10): 4090-100.

27. Farhat D, Lincet H. Lipoic acid a multi-level molecular inhibitor of tumorigenesis. Biochim Biophys Acta Rev Cancer. 2020;1873(1):188317.

28. Liu D, Heij LR, Czigany Z, Dahl E, Lang SA, Ulmer TF, Luedde T, Neumann UP, Bednarsch J. The role of tumor-infiltrating lymphocytes in cholangiocarcinoma. J Exp Clin Cancer Res. 2022 Apr 7;41(1):127.

29. Goeppert B, Frauenschuh L, Zucknick M, Stenzinger A, Andrulis M, Klauschen F, et al. Prognostic impact of tumour-infiltrating immune cells on biliary tract cancer. Br J Cancer. 2013;109(10):2665–2674.

30. Asahi Y, Hatanaka KC, Hatanaka Y, Kamiyama T, Orimo T, Shimada S, et al. Prognostic impact of CD8+ T cell distribution and its association with the HLA class I expression in intrahepatic cholangiocarcinoma. Surg Today. 2020;50(8):931–940.

31. Kim HD, Kim JH, Ryu YM, Kim D, Lee S, Shin J, et al. Spatial Distribution and Prognostic Implications of Tumor-Infiltrating FoxP3- CD4+ T Cells in Biliary Tract Cancer. Cancer Res Treat. 2021;53(1):162–171.

32. Zhou G, Sprengers D, Mancham S, Erkens R, Boor PPC, van Beek AA, et al. Reduction of immunosuppressive tumor microenvironment in cholangiocarcinoma by ex vivo targeting immune checkpoint molecules. J Hepatol. 2019;71(4):753–762.

33. Yue L, Ren Y, Yue Q, Ding Z, Wang K, Zheng T, et al. α-Lipoic Acid Targeting PDK1/NRF2 Axis Contributes to the Apoptosis Effect of Lung Cancer Cells. Oxid Med Cell Longev. 2021;2021:6633419.